Effects of molecule hydrophobicity and structural flexibility of appended bispecific antibody on Protein A chromatography

Q1Q2

The corrections made in this section will be reviewed and approved by a journal production editor.

Xinhui Wang[a,1], Nattha Ingavat[a,1], Jia Min Liew[a], Nuruljannah Dzulkiflie[a], Han Ping Loh[b], Yee Jiun Kok[c], Xuezhi Bi[c], Yuansheng Yang[b], Wei Zhang[a,*], zhang_wei@bti.a-star.edu.sg

[a]Downstream Processing, Bioprocessing Technology Institute (BTI), Agency for Science, Technology and Research (A*STAR), 20 Biopolis Way, #06-01 Centros, Singapore 138668, Singapore

[b]Cell Line Development, Bioprocessing Technology Institute (BTI), Agency for Science, Technology and Research (A*STAR), 20 Biopolis Way, #06-01 Centros, Singapore 138668, Singapore

[c]Analytical Science & Technology (Protein Analytics), Bioprocessing Technology Institute (BTI), Agency for Science, Technology and Research (A*STAR), 20 Biopolis Way, #06-01 Centros, Singapore 138668, Singapore

*Corresponding author.

[1]These two authors contributed equally to this work.

Abstract

Appended bispecific antibody (aBsAb) with two single chain variable fragments (scFv) linked at the c-terminus of its heavy chains is one of the promising formats in bispecific therapeutics. The presence of hydrophobic and flexible scFv fragments render aBsAb molecules higher molecule hydrophobicity and structural flexibility compared to monoclonal antibody (mAb), thus making its purification more challenging. We set out to investigate how the unique molecular properties of aBsAb affect its performance on Protein A chromatography. We showed that aBsAb has a high propensity for chromatography-induced aggregation due to its high molecule hydrophobicity, and this couldn't be improved by the addition of common chaotropic salts. Moreover, the presence of chaotropic salts, such as arginine hydrochloride (Arg-HCl), retarded aBsAb elution during Protein A chromatography rather than facilitating which was widely observed in mAb Protein A elution. Nevertheless, we were able to overcome the aggregation issue by optimizing elution condition and improved aBsAb purity from 29 % to 93 % in Protein A eluate with a high molecular weight (HMW) species of less than 5 %. We also showed that the high molecular flexibility of aBsAb leads to different hydrodynamic sizes of the aBsAb molecule post Protein A elution, neutralization, and re-acidification, which are pH dependent. This is different from mAbs where their sizes do not change post neutralization even with re-exposure to acid. The above unique observations of aBsAb in Protein A chromatography were clearly explained from the perspectives of its high molecular hydrophobicity and structural flexibility.

Keywords:

Appended bispecific antibody (aBsAb); Single-chain variable fragment (scFv); Molecule hydrophobicity; Structural flexibility; Protein A chromatography; Chromatography-induced aggregation

Data availability

No data was used for the research described in the article.

Abbreviations

aBsAb appended bispecific antibody

BsAb bispecific antibody

mAb monoclonal antibody
Arg-HCl arginine hydrochloride
HMW high molecular weight
LMW low molecular weight
scFv single-chain variable fragment
HC heavy chain
LC light chain
CV column volume
GS glycine-serine
HCCF harvested cell culture fluid
DBC dynamic binding capacity
RT residence time
VH heavy chain variable domain
VL light chain variable domain
SD ~~S~~standard deviation

1 Introduction

Bispecific antibodies (BsAb) are engineered proteins which can recognize two different antigens on their binding arms, usually targeting cancer cells and the other arm targeting immune cells such as the T-Cells and NK cells simultaneously, potentially leading to increased drug efficacy and safety [1]. With the recent FDA approval for multiple bispecifics such as Talvey, for multiple myeloma, Epkinly and Columvi for B-cell lymphomas and Vabysmo for treatment of neovascular age-related macular degenerated and diabetic macular edema [2,3], BsAb is becoming a fast growing field with many more lined up for regulatory review in the coming years [2].

Currently, there are more than 100 different formats of BsAb reported [4,5]. These wide variety of BsAb formats are specifically designed in order to match their proposed mechanisms and intended uses. The appended bispecific antibody (aBsAb) represents a highly intriguing format within the realm of bispecific antibodies. Cadonilimab, an aBsAb, has been recently approved in China for the treatment of metastatic cervical cancer [6]. Additionally, at least 19 bsAb molecules of this format are currently undergoing clinical trials [7]. This evidence demonstrates the potential of this bsAb format as a new therapeutic, hence opening new possibilities for treating a range of diseases, including cancer and autoimmune disorders. These artificial, large molecules feature a flexible linker that connects the framework IgG to the single-chain variable fragments (scFv). Typically, glycine-serine (GS) peptides serve as conventional linkers, chosen for their short side chains, which allow for flexibility of the scFv to effectively bind to their target antigen site [8]. However, aBsAb have higher hydrophobicity, primarily attributed to the inclusion of two additional hydrophobic scFv domains, leading to a notable tendency for aggregation [9-11]. Moreover, the incorporated linkers may introduce significant structural flexibility to the molecule. These characteristics present challenges in the purification process [8,12]. As aBsAb retains IgG structure, it is presumed to be amenable to Protein A chromatography as an affinity capture step, akin to the process employed for its parental monoclonal antibody (mAb). Nevertheless, purification using the conventional Protein A method for aBsAb has been reported to yield sub-optimal results, characterized by low yields and purity [13,14].

In this paper, we worked on a model aBsAb, with the framework IgG, Trastuzumab, with two anti-CD16 scFvs linked at the c-terminus of heavy chains (Fig. 1). Here we investigate how this highly hydrophobic and structurally flexible aBsAb performs on Protein A chromatography. We not only showed that aBsAb exhibited strong aggregation tendency on the Protein A column due to its highly hydrophobic nature but addition of chaotropic salt, namely arginine hydrochloride (Arg-HCl) hindered its elution contrary to its traditional effect on mAb elution. The flexibility of the aBsAb also rendered its hydrodynamic radius to change post elution neutralization and reacidification. This observation is unique and different from mAbs. With this new understanding of the aBsAb, there can be further improvements in designing the aBsAb molecule or to design the purification process to minimize its aggregation and stability issues.

Images may appear blurred during proofing as they have been optimized for fast web viewing. A high quality version will be used in the final publication. Click on the image to view the original version.

alt-text: Fig 1

Fig. 1

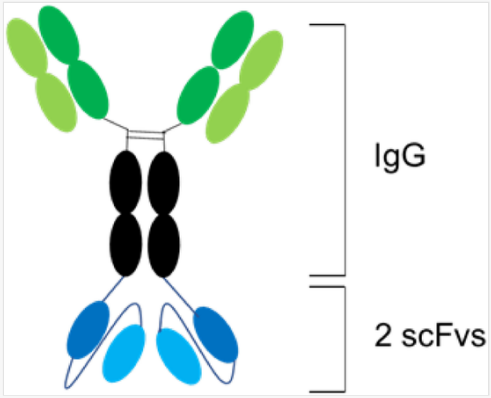

Structure of the model aBsAb investigated in this study. Framework IgG Trastuzumab linked to 2 scFvs (blue) at the c-terminus with 2 flexible glycine-serine peptide linkers.

2 Materials and methods

2.1 BsAb culture

Stably transfected CHO K1 cell lines producing aBsAb targeting HER2 and CD16 were generated by site-specific integration of plasmid vectors, which carried genes encoding trastuzumab light chain (LC), trastuzumab heavy chain (HC) coupled to anti-CD16 scFv. The cDNAs for trastuzumab heavy chain variable domain (VL) and light chain variable domain (VH) were designed using the amino acid sequences of trastuzumab found in the international ImMunoGeneTics information system (IMGT). The cDNAs for CD16 were reversely transcribed from amino acid sequences from a previous study [15]. For the targeted molecule, the VH and VL in scFv were connected through a flexible linker (G4S)3, which was further linked to the C- terminus of the HC through a (G4S)2 linker.

Stably transfected pools were generated through recombinase-mediated cassette exchange (RMCE) by co-transfecting CHO K1 master cells with an appropriate targeting vector expressing a bispecific antibody and a vector expressing FLPe. A comprehensive protocol for the creation of stably transfected pools and their subsequent production in fed-batch cultures has been detailed in our prior study [16]. Briefly, following stable transfection, the cell lines were cultured in EX-CELL® Advanced CHO Fed-batch Medium (SAFC, Sigma) and supplemented with 6 mM glutamine (Sigma) in 50 mL tubespin (TPP). The cultures were then placed in a Kuhner shaker (Adolf Kühner AG) with 8 % CO_2 at 37 °C under humidified conditions. To produce the desired molecule, 300 mL of cell culture with a viable cell density of 3×10^5 cells/mL were inoculated into 600 mL tubespin (TPP) in the same humidified Kuhner shaker (Adolf Kühner AG) with 8 % CO_2 at 37 °C. On days 3, 5, 7, 9, and 11, 30 mL of Ex-Cell Advanced CHO Feed 1 (with glucose) (SAFC, Sigma) was introduced. The Vi-Cell XR Viability Analyzer (Beckman Coulter) was employed for evaluating cell density and viability at days 3, 5, 7, 9, 11, and 14. The concentration of D-Glucose in the culture medium was determined using the Nova BioProfile 100 Plus Analyzer (Nova Biomedical). If the glucose concentration in the media fell below 2 g/L, D-glucose (Sigma) was introduced to raise the concentration above 6 g/L. On day 14, the culture supernatant was gathered, underwent centrifugation, and was filtered to eliminate cells and cell debris before proceeding with the purification process.

2.2 AKTA chromatography

A 1 mL MabSelect™ PrismA columns (Cytiva) was packed using a Tricorn™ 5 column to a bed height of 5.1 cm. All PrismA chromatographic experiments were performed on an AKTA™ Avant 25 (Cytiva). PrismA column was equilibrated with 100 mM sodium phosphate, 150 mM the sodium chloride (NaCl), pH 7.2 (5 column volume (CV)), before loading the appropriate amount of harvested cell culture fluid (HCCF). A 5 CV wash of 100 mM sodium phosphate, 150 mM NaCl, pH 7.2 was performed after loading of HCCF followed by 10 CV wash of 50 mM sodium citrate, pH 4.0 for all experiments. Elution was performed with elution buffers contain 25 mM sodium acetate, 25 mM glycine with or without 100 mM arginine hydrochloride (Arg-HCl) at their respective pH between 3.6 and 3.0 (8 CV). For the NaCl experiment, the elution buffer used was 25 mM sodium acetate, 25 mM glycine with 100 mM NaCl, pH 3.6. The column was further stripped with 100 mM glycine, pH 2.5 for 10 CV and re-equilibrated with 100 mM sodium phosphate, 150 mM NaCl, pH 7.2 (2 CV). The column is then clean-in-place (CIP) with 1 M NaOH (3 CV), re-equilibrated with 100 mM sodium phosphate, 150 mM NaCl, pH 7.2 (8 CV) and stored in 20 % Ethanol (4 CV). The eluates were adjusted to pH 6.5 using 1 M Tris pH 8.0 or 100 mM glycine, pH 2.5 prior to subsequent analysis.

For the stability studies, the eluates were adjusted to between pH 2.8 to pH 3.8 using either 100 mM glycine, pH 2.5 or 1 M Tris, pH 8.0. The samples were held up to 4 h before neutralized back to pH 6.5 and analyzed on the size exclusion-high-performance liquid chromatography (SEC—HPLC).

Dynamic Binding Capacity (DBC) experiment was performed using the same 1 mL MabSelect™ PrismA column and loaded to 100 % breakthrough with the HCCF with a residence time of 2.5 mins. The flowthrough was collected in fractions and analyzed by SEC—HPLC to obtain the estimated monomeric aBsAb breakthrough in each fraction. A graph of the breakthrough percentage to the total monomer loaded was plotted and the DBC of the aBsAb was determined at 10 % breakthrough.

A pH gradient elution experiment was performed using a 1 mL MabSelect™ PrismA column. The column was equilibrated with 100 mM sodium phosphate, 150 mM NaCl, pH 7.2 (5 CV), loaded with HCCF, washed with 100 mM sodium phosphate, 150 mM NaCl, pH 7.2 (5 CV), and elution was performed using 2 buffers to create a gradient: Buffer A, 50 mM sodium citrate, pH 6, and Buffer B, 50 mM sodium citrate, pH 3, in 30 CV with a further 10 CV hold at 100 % Buffer B. The eluate was collected in 1 mL fractions. The column was then re-equilibrated with 100 mM sodium phosphate, 150 mM NaCl, pH 7.2 (2 CV), CIP with 1 M NaOH (3 CV), re-equilibrated with 100 mM sodium phosphate, 150 mM NaCl, pH 7.2 (3 CV) and stored in 20 % Ethanol (4 CV).

The validation runs were carried out using a 24 mL MabSelect™ PrismA column (XK16; Cytiva), using the same buffers as above AKTA experiments.

All HCCF load were 0.2 μm filtered prior to loading onto the column and prior to SEC analysis. The pH values of collected eluates and buffers were measured using an external pH probe (Mettler Toledo), where necessary. All buffers, salts and reagents were purchased from Merck Millipore.

2.3 aBsAb concentration and purity analysis

The aBsAb concentration and purity were analyzed by SEC—HPLC using a TSKgel G3000SWXL column (7.8 mm i.d. x 30 cm; Tosoh Bioscience) with a flow rate of 0.6 mL/min. A TSKgel guard column SWXL (6.0 mm i.d. x 4 cm; Tosoh Bioscience) is placed before the main SEC column. The mobile phase consisted of 0.2 M L-arginine, 0.05 M MES, 5 mM EDTA, 0.05% sodium azide (w/w), pH 6.5. The UV absorbance was monitored at 280 nm. aBsAb concentrations were quantified using the area under the peaks, referenced to a calibration curve generated using antibody standards with known concentrations and corrected for using the respective extinction coefficient. The aBsAb titer in HCCF was also quantified using SEC—HPLC, as it could accurately reflect the concentration of monomer. The aBsAb titer was calculated by subtracting monomeric peak integration of HCCF from that of the flowthrough from PrismA chromatography. This ensures that the other proteins in the HCCF are excluded from the titre calculation. The amount of aggregates and fragments present in the sample was calculated using the area of peaks eluting before and after the monomeric peak respectively.

2.4 Dynamic light scattering analysis

The dynamic light scattering (DLS) experiments were performed using the Zetasizer Ultra (Malvern Instruments). Each sample was 0.22 μm filtered and loaded into a disposable micro cuvette and measured at 25 °C. The intensity-based size measurements were obtained using cumulant analysis. The eluate sample from the validation runs were measured just after elution at pH 3.4, neutralized to pH 6.5 and re-acidified to pH 3.4. Further studies using the neutralized pH 6.5 eluate samples were performed by adjusting the pH to between pH 3.0 to pH 5.0 using 100 mM glycine, pH 2.5 and these samples were measured on the DLS. At least three independent replicates of each sample were measured to reduce statistical uncertainties in the results.

2.5 Intact mass analysis

Intact mass analysis was performed by LC-MS as previously described [17]. Briefly, the sample from each SEC—HPLC fraction with 200 ng total protein was acidified with 0.3 % formic acid and analysed using a BioResolve RP mAb Polyphenyl column on a nanoACQUITY UPLC (Waters) coupled to a TripleTOF 6600 MS (SCIEX). Mass spectra were processed and deconvoluted using PMI-Byos v5.2.31 Intact Mass™ workflow (Protein Metrics Inc.).

3 Results

3.1 Stability study of the aBsAb at low pH

Anticipating a high aggregation propensity of aBsAb due to the presence of two scFv domains in the molecule, we first incorporated a stability study into our purification development. Protein A chromatography was first conducted with a gradient elution ranging from pH 6.0 to pH 3.0 to determine the elution pH range for the aBsAb. Observing that aBsAb was eluted at pH 3.1 - 3.5 (Fig. 2), we selected a pH range of 2.8 - 3.8, with an increment of 0.2 units, to cover the eluate pH range for our stability study. The study was structured to mirror the workflow following Protein A chromatography, where the low pH hold (for viral inactivation) and subsequent neutralization steps to pH 6.5 were to be carried out.

Images may appear blurred during proofing as they have been optimized for fast web viewing. A high quality version will be used in the final publication. Click on the image to view the original version.

alt-text: Fig 2

Fig. 2

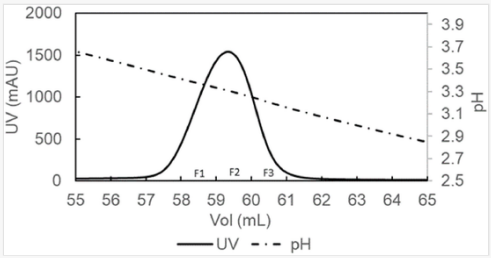

Chromatogram of PrismA pH gradient elution. The aBsAb eluate eluted in the range of pH 3.1 to pH 3.5. The eluates were collected in 1 mL fractions. F1, F2 and F3 were collected and sent for intact mass analysis.

Notably, when aBsAb was held at pH 2.8, there was a marked decrease in protein purity, accompanied by an increase in both low molecular weight (LMW) and high molecular weight (HMW) species after neutralization (Fig. 3). In contrast, holding the aBsAb within the pH range of 3.8 to 3.0 resulted in monomer purity remaining above 90 %, post-neutralization. These findings suggested that the molecule remained stable after being acidified within the pH range of 3.0 to 3.8.

Images may appear blurred during proofing as they have been optimized for fast web viewing. A high quality version will be used in the final publication. Click on the image to view the original version.

alt-text: Fig 3

Fig. 3

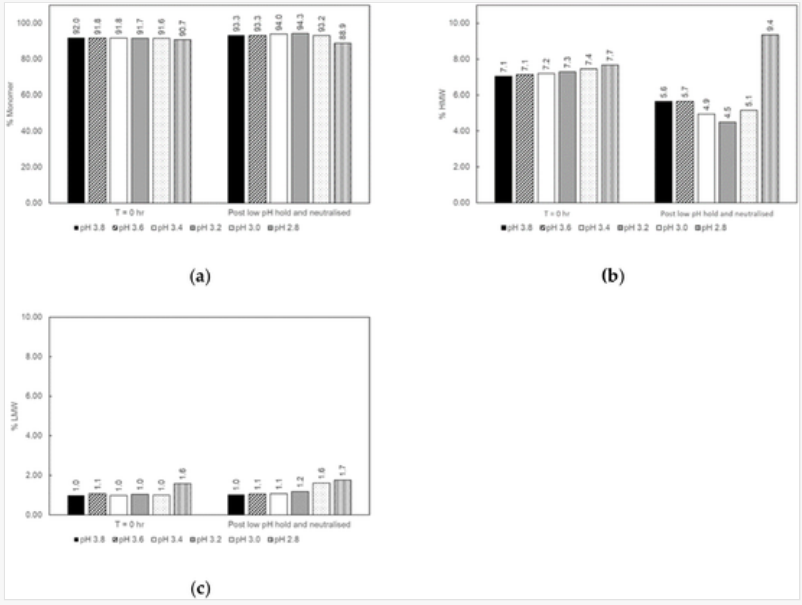

Stability assessment of aBsAb during low pH hold, followed by neutralization. The purity of the samples was analyzed using SEC—HPLC right after Protein A elution ($T = 0$ hr) and post low pH hold and neutralised respectively. The graphs illustrate (a)%Monomer, (b)%High Molecular Weight (HMW), and (c)%Low Molecular Weight (LMW).

Interestingly, there was a noticeable reduction in HMW species after neutralization for all pH levels, except at pH 2.8, indicating a potential reversible aggregation phenomenon post-neutralization for this aBsAb. Although pH 3.8 maintained decent protein purity post-neutralization, it was excluded from the subsequent experiment due to the anticipated low recovery. Ultimately, we opted for a pH range of 3.0 to 3.6 for the subsequent set of experiments to determine the optimal Protein A elution pH for aBsAb.

3.2 Investigation of optimal elution conditions for aBsAb during the Protein A chromatography

3.2.1 Screening for an optimal elution pH

The optimal Protein A chromatography elution pH for the aBsAb was determined using elution buffers composed of 25 mM sodium acetate and 25 mM glycine at pH values of 3.0, 3.2, 3.4, and 3.6 respectively. This sodium

acetate/glycine mixture was selected based on reported suitability for maintaining consistent buffering capacity within our specified pH range of interest (pH 3.0 to 3.6) [10]. Step elution was performed with these buffers.

In terms of recovery, monomeric yields were calculated for evaluation, with elution at pH 3.4 resulting in the highest monomeric yield of 88.6 % among all tested pH conditions (Fig. 4). Despite the expectation of higher yields with elution at pH 3.2 and pH 3.0, they showed similar yields (80.1 % for pH 3.2; 80.0 % for pH 3.0), both of which were lower than the yield achieved at pH 3.4. These lower yields were likely due to potentially elevated levels of chromatography-induced aggregates at the lower pH, leading to the alteration of the aBsAb monomers to aggregates, which remained tightly bound to the column during elution, with subsequent release occurring only during the CIP step. This speculation was supported by the comparison of CIP peaks, where there were higher peaks for pH 3.0 and pH 3.2 compared to pH 3.4 (Fig. 5). Finally, elution at pH 3.6 yielded the lowest recovery rate (69.1 %), aligning with the expected trend for a gentler pH during Protein A elution.

Images may appear blurred during proofing as they have been optimized for fast web viewing. A high quality version will be used in the final publication. Click on the image to view the original version.

alt-text: Fig 4

Fig. 4

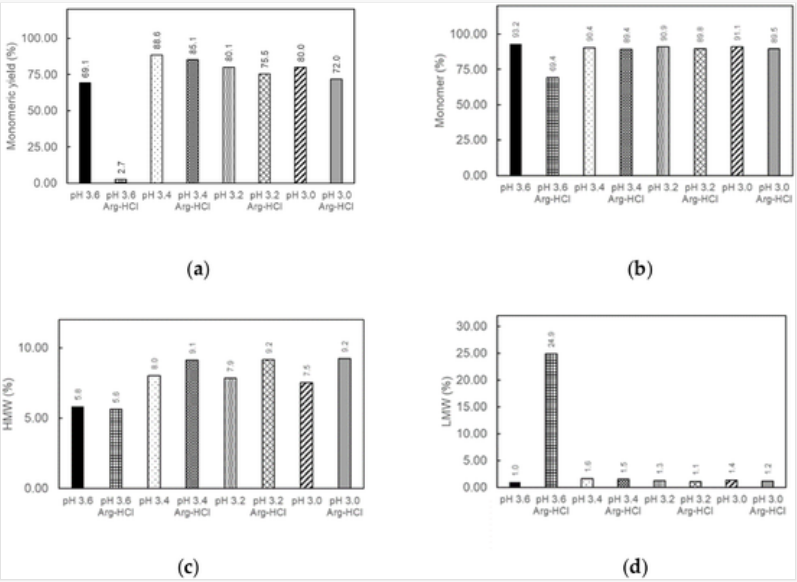

The neutralized aBsAb eluate (a)%Monomeric yield, (b)%Monomer, (c)%HMW, (d)%LMW obtained in the presence with and without Arg-HCl at varying pH conditions from pH 3.0 to pH 3.6 for Protein A chromatography elution.

Images may appear blurred during proofing as they have been optimized for fast web viewing. A high quality version will be used in the final publication. Click on the image to view the original version.

alt-text: Fig 5

Fig. 5

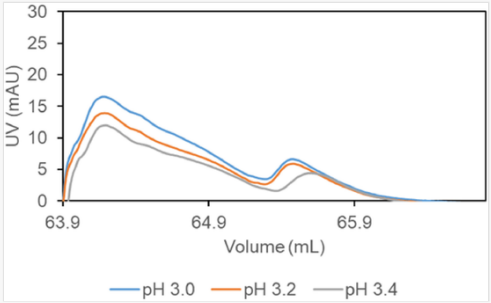

CIP peak results for experiments of elution buffers pH 3.4, pH 3.2 and pH 3.0. pH 3.0 has the highest area under the curve followed by pH 3.2 and the least being pH 3.4.

Regarding monomer purity, all elution buffers consistently achieved a purity higher than 90 %. Notably, pH 3.6 yielded the highest purity at 93.2 %, potentially attributable to improved resolution between the monomer and HMW species at a higher elution pH. Elution within the pH range of 3.0 to 3.4 resulted in similar product purity, with%Monomer of 90.4 % (pH 3.4); 90.9 % (pH 3.2), and 91.1 % (pH 3.0), respectively. pH 3.4 was identified as the optimal pH for the elution buffer due to its outstanding yield and good purity.

3.2.2 Addition of arginine hydrochloride (Arg-HCl) to the elution buffer, aiming to mitigate chromatography-induced aggregation

As the HMW contents persisted at elevated levels in the post-Protein A products across all tested elution pH values, further optimization was pursued by introducing 100 mM Arg-HCl into the elution buffer. Arg-HCl is conventionally utilized in purification processes to facilitate antibody dissociation from ligands and suppress aggregation during chromatography. However, contrary to expectations, we observed a retardation of the elution peaks at all elution pH values, with complete peak retardation at the elution pH of 3.6 in the presence of Arg-HCl. In this instance, the elution peak only emerged during the subsequent glycine strip wash (100 mM glycine, pH 2.5) (Fig. 6a), and its identity was confirmed to be monomers rather than HMWs through SEC—HPLC (Fig. 6b). The retardation using elution buffer containing 100 mM NaCl, pH 3.6 was less as comparatively to that using 100 mM Arg-HCl, pH 3.6, eluting in the elution phase. Furthermore, there was a broadening of the elution peak at each respective elution pH value compared to the controls (elution buffers without Arg-HCl).

Images may appear blurred during proofing as they have been optimized for fast web viewing. A high quality version will be used in the final publication. Click on the image to view the original version.

alt-text: Fig 6

Fig. 6

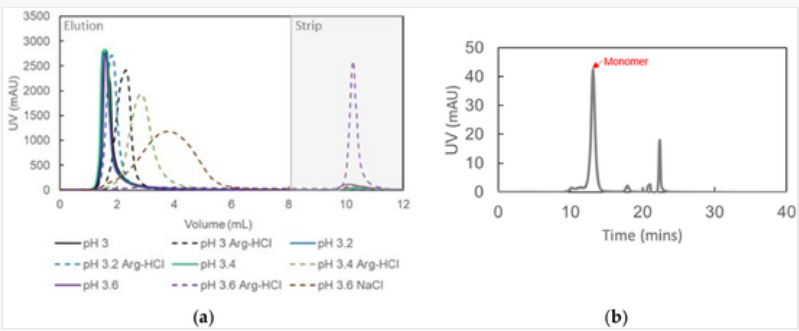

(a). AKTA chromatograms of the elution peak at varying elution pH in the presence and absence of Arg-HCl. All eluates eluted during the elution phase, except for pH 3.6 Arg-HCl, which mainly eluted in the strip phase. (b) SEC—HPLC results showed that majority of the strip peak from pH 3.6 Arg-HCL experiment were monomers.

Upon comparing product yields, it was evident that the overall yields were lower for all pH values after the addition of Arg-HCl, associated with drops in overall purity. For pH 3.4 to pH 3.0,%HMW increased by at least 1 % after incorporating Arg-HCl in the elution buffer (Fig. 4). The LMW contents continued to elute during the elution phase and remained at approximately less than 2 % in the products for most elution pH values, except for pH 3.6 with Arg-HCl, exhibiting a comparatively high level of LMW contents as the monomer was fully retarded and eluted during the glycine strip wash phase. Consequently, we determined that Arg-HCl is not suitable to be included in the elution buffer for this aBsAb molecule, as it did not improve both product yield and purity. As a consequence, the optimal elution buffer for this aBsAb would be 25 mM sodium acetate, 25 mM glycine, pH 3.4.

3.3 Investigation of loading density and loading residence time effects

3.3.1 Loading density

Protein A runs were conducted at two distinct aBsAb mass loads (90 % and 50 % QB10) to determine the effects of loading density on the purity and yield of the aBsAb. Before that, the dynamic binding capacity (DBC) of aBsAb for the MabSelect™ PrismA resin at a 10 % breakthrough with a loading residence time (RT) of 2.5 mins was determined (QB10 = 40 mg/mL). Subsequently, the column was loaded at 90 % and 50 % QB10.

As expected, the yield was lower at 90 % QB10 loading compared to 50 % QB10 loading (74.7 % at 90 % QB10; 87.8 % at 50 % QB10) (Fig. 8), with 8 % of monomeric aBsAb loss during the post-load-wash (Fig. 7). However, the difference in product purity was minimal, and HMW% in the product pools in 90 % QB10 run (10.7 %) was only slightly higher than 50 % QB10 run (10.1 %). This raised the question that a higher loading density may not be the single driving force behind aggregation during chromatography; instead, it could potentially also be due to the interaction duration of aBsAb and the Protein A resin. Therefore, we conducted further experiments to investigate the effect of loading residence time on the degree of chromatography-induced aggregation.

Images may appear blurred during proofing as they have been optimized for fast web viewing. A high quality version will be used in the final publication. Click on the image to view the original version.

alt-text: Fig 7

Fig. 7

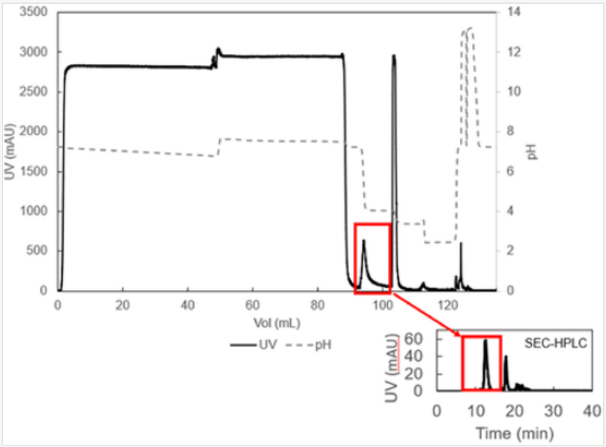

AKTA chromatogram of the 90 % QB10 runs at a loading residence time of 2.5 mins. The peak indicated in the chromatogram came out during the wash step and is predominantly the monomer as confirmed via SEC—HPLC (insert).

Images may appear blurred during proofing as they have been optimized for fast web viewing. A high quality version will be used in the final publication. Click on the image to view the original version.

alt-text: Fig 8

Fig. 8

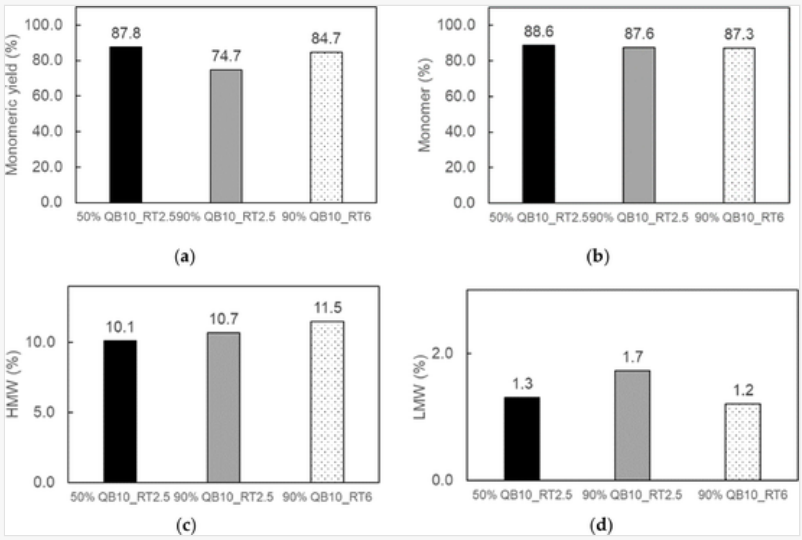

The aBsAb eluate (a)%Monomeric yield, (b)%Monomer, (c)%HMW, (d)%LMW with varying loading conditions and residence time (RT) of 2.5 mins and 6 mins. QB10 was determined at 2.5 mins RT.

3.3.2 Residence time

We then set out to further investigate if increasing the loading residence time on the column would affect the chromatography-induced aggregation. We performed another set of experiment loading aBsAb at 90 % QB10 (determined at 2.5 mins) with a residence time of 6 mins. Yield was increased due to the higher residence time, and HMW% also further increased slightly by 0.8 %, suggesting that increasing the interaction time for the aBsAb with Protein A resin could have contributed to higher chromatography-induced aggregation (Fig. 6). The increase in HMW may not be significantly higher due to usage of the optimal pH 3.4 for the elution buffer. In summary, at an optimal pH of 3.4, increasing loading density and residence time did not significantly affect product purity nor chromatography-induced aggregation.

3.3.3 Protein A chromatography scale-up

To validate the performance of the Protein A chromatography process, we used a 24 mL XK16 column and loaded it to 20 mg/mL (50 % QB10 RT 2.5 mins) and eluted the aBsAb using 25 mM sodium acetate, 25 mM glycine pH 3.4. The eluate achieved a purity of 93.0 % and the recovery was 88.8 % (Table 1). This shows that the process is robust when scaled up.

alt-text: Table 1

Table 1

The table layout displayed in this section is not how it will appear in the final version. The representation below is solely purposed for providing corrections to the table. To view the actual presentation of the table, please click on the Preview located at the top of the page.

Results from the Protein A validation run on XK16 column with 50 % QB10 RT 2.5 mins.

Sample	Recovery (%)	Purity		
		HMW (%)	Monomer (%)	LMW (%)
HCCF	–	27.10	29.16	43.74
Protein A Eluate (Post Neutralisation)	88.8	4.2	93.0	2.8

3.4 Investigation of aBsAb structure flexibility

3.4.1 Hydrodynamic radius changes of aBsAb molecule post Protein A chromatography

The Protein A eluate from the scale-up validation run was measured using dynamic light scattering (DLS). It was noticed that the sample post neuturalization to pH 6.5 was large around 18 to 19 nm (Fig. 9), which is almost twice the size of typical mAbs which are approximately 10 to 11 nm [18]. In a previous study performed by Gagnon et al. [19,20], it was noticed that the hydrodynamic radius of the IgG may decrease to 5.5 nm during elution, and we further investigated this phenomenon using aBsAb. We noted that the hydrodynamic radius was the smallest when it was first eluted and increased when neutralized back to pH 6.5 (Fig. 9). When the sample was reacidified to pH 3.4 again, there

was a reduction in the hydrodynamic radius, which is different from mAbs where there is no change in the hydrodynamic radius once the sample was acidified after adjustment to physiological pH.

Images may appear blurred during proofing as they have been optimized for fast web viewing. A high quality version will be used in the final publication. Click on the image to view the original version.

alt-text: Fig 9

Fig. 9

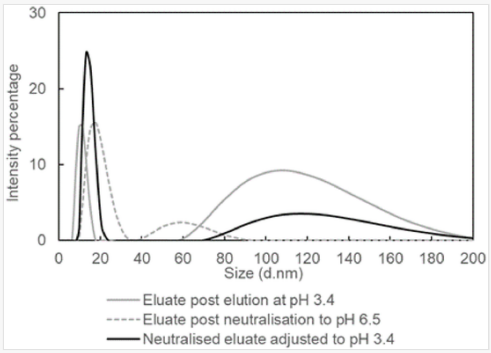

DLS results illustrating the size distribution of the eluates against the intensity percentage for the scale-up validation run. The eluate was measured on the DLS once it eluted, after neutralization to pH 6.5 and again after re-acidification to pH 3.4.

We further tested the neutralized eluate sample by adjusting its pH from 3 to 5 and measured the corresponding hydrodynamic radius. The results showed that the bsAb molecule size is the smallest at pH 3 and increases as the pH increases, indicating that the size of the aBsAb molecule is pH dependent (Fig. 10, Table 2).

Images may appear blurred during proofing as they have been optimized for fast web viewing. A high quality version will be used in the final publication. Click on the image to view the original version.

alt-text: Fig 10

Fig. 10

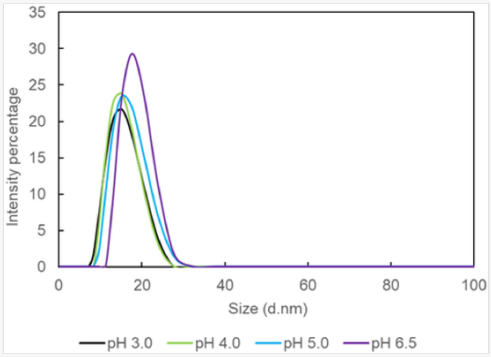

Hydrodynamic radius of the neutralized aBsAb eluate (pH 6.5) adjusted to the different pH from pH 3 to pH 5 and subsequently measured using DLS. The hydrodynamic radius of the aBsAb was noted to increase as the pH increases.

alt-text: Table 2

Table 2

The table layout displayed in this section is not how it will appear in the final version. The representation below is solely purposed for providing corrections to the table. To view the actual presentation of the table, please click on the Preview located at the top of the page.

Hydrodynamic radius of the aBsAb at different pH.

pH	Hydrodynamic radius (nm)
3	15.0
4	15.0

5	16.4
6.5 (neutralized eluate, original sample)	18.9

3.4.2 SEC—HPLC split peak and peak ratio differences of Protein A eluate

During the initial pH gradient elution experiment we collected the eluate in 1 mL fractions, F1 to F3 (Fig. 2). Upon analysing the eluate fractions on SEC—HPLC, we noticed that the different eluate fractions had different split peak ratio profiles (Fig. 11). These fractions were sent for mass spectrometry analysis and ran on non-reducing SDS-gel, which revealed that all these fractions had the same intact mass (Supplementary Figures 1 and 2). This suggests that the split peak observed in the SEC profile is likely due to the presence of different molecular conformations of the aBsAb molecule, potentially attributable to the high structural flexibility conferred by the two appended scFv domains.

Images may appear blurred during proofing as they have been optimized for fast web viewing. A high quality version will be used in the final publication. Click on the image to view the original version.

alt-text: Fig 11

Fig. 11

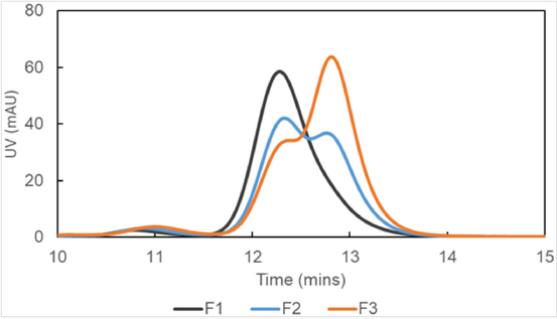

SEC—HPLC results from the different fractions from Protein A pH gradient run. The SEC profile shows the split peaks from the different fractions F1, F2 and F3.

4 Discussion

4.1 Effects of high molecule hydrophobicity of aBsAb on Protein A chromatography

Antibodies bind to Protein A column mainly through hydrophobic interactions as well as hydrogen bonding and ionic interactions [21-23]. Hydrophobic interactions are also known to be the most critical non-covalent forces driving the formation of protein aggregates [24]. In a previous study [25], the authors showed that reducing the hydrophobicity of the mAb by point mutation helped to significantly improve the aggregation propensity of the molecule. The incorporation of the two scFvs into the aBsAb significantly enhances the molecule's hydrophobicity compared to its parental antibody. For reference, the grand average of hydropathicity (GRAVY) was computed (https://web.expasy.org/protparam) to compare molecular hydrophobicity. The GRAVY of aBsAb is −0.406, of scFv is −0.357, and of its parental monoclonal antibody (Herceptin) is −0.423, suggesting that the installation of the two scFv domains significantly contributes to the increased molecular hydrophobicity of aBsAb, as a less negative GRAVY indicates higher hydrophobicity. Hence, the GRAVY values support that aBsAb is more hydrophobic than the parental Herceptin. This change consequently impacts the aBsAb's performance on the Protein A column leading to its propensity to aggregate under stress conditions including low pH or it may also enhance the hydrophobic interaction to the column.

Firstly, our study illustrated that the interactions of the aBsAb with the Protein A likely led to increased chromatography-induced aggregation at lower pH. When exposed to stress conditions such as lower pH during elution on column (pH 3.0 and pH 3.2), the yield dropped, which is counterintuitive as lower pH should be able to eluate more aBsAb from the column. Our stability study also demonstrated that the aBsAb is stable at these two low pH values. Upon closer inspection, we gathered that the lower pH had caused more chromatography-induced aggregation, leading to the strongly bound aggregate to only elute during the strip phase. This suggests that interactions of aBsAb with Protein A can introduce more instability to this bsAb, leading to increased aggregation. It is likely that the aBsAb may experience more hydrophobic attractions between each other as well as the Protein A column, driving self-association during chromatography.

Secondly, we observed the increase of residence time together with increasing loading density led to higher aggregation. The binding of antibodies to the Protein A column is known to cause conformational changes [19,20,26],

which may expose the hydrophobic regions on the aBsAb. A longer residence time would render the destablised aBsAb a longer time to interact, leading to increased aggregation. Additionally, a higher concentration of aBsAb in the column denoted with the high load density would also allow for a higher probability of the destablised antibodies to interact with each other, leading to aggregation.

Thirdly, we observed the higher hydrophobicity of the aBsAb molecule led to enhanced retention on the Protein A column in the presence of Arg-HCl. While attempting to mitigate chromatography-induced aggregation by adding Arg-HCl to the elution buffer, we noted that aBsAb elution was retarded rather than facilitated. This is contrary to the effect of Arg-HCl in the Protein A elution buffer for mAbs [27-29]. Protein elution with NaCl at pH 3.6 also resulted in a delayed elution peak, but it was not as pronounced as with Arg-HCl, suggesting that other interactions offered by the guanidinium group on Arg-HCl also significantly contribute to the retardation, potentially through the enhancement of aBsAb hydrophobicity in the presence of Arg-HCl.

It is noteworthy that while low pH conditions can mitigate protein-protein interactions (PPI) among aBsAb molecules by causing repulsive positively charged interactions, they can also compromise structural flexibility and stability, potentially leading to partial protein unfolding and promoting aggregation [30,31]. This effect is especially pronounced when the protein is highly hydrophobic and highly concentrated on the Protein A sorbents.

A previous study reported that Arg-HCl can interact with aromatic residues on protein surfaces through π-cation interactions, affecting conformational stability [23]. π-cation interactions are particularly relevant on potential hydrophobic surfaces, influencing hydrophobic interactions and potentially leading to protein aggregation. Given the presence of two scFv domains in aBsAb, which introduce extra hydrophobic patches, Arg-HCl could potentially enhance the exposure of these hydrophobic patches, making the aBsAb molecule more hydrophobic during Protein A chromatography. As a result, the overall outcomes are a retardation of the elution peak and an increased propensity for aggregation, as evidenced in our study.

A similar phenomenon had been previously noted during Protein L chromatography when purifying a tandem scFv with high molecule hydrophobicity as well [32]. Our observation during Protein A chromatography for the aBsAb purification was consistent with the evidence from Protein L, suggesting a strengthening effect between the aBsAb and the Protein A ligand in the presence of arginine. This is contrary to common previous findings where arginine typically facilitates the dissociation of the antibody from Protein A.

Interestingly, there was no improvement in the yield and purity of the eluate. In fact, it was noted that eluates with Arg-HCL in the elution buffer led to higher HMW percentage. As previously reported, the effects of Arg-HCl on aggregation of mAb is largely molecule dependent and may even increase aggregation [23,33]. Arginine can engage with proteins through multiple binding mechanisms. One such way is through electrostatic interactions, where its positively charged guanidinium group interacts with negatively charged residues on the protein surface. Apart from electrostatic interactions, arginine can also participate in cation-π interactions with aromatic residues on proteins and establish hydrogen bonds with proteins [34]. The presence of Arg-HCl in the elution buffer could have affected the colloidal stability of the aBsAb, increasing protein-protein interaction of the aBsAb via the exposed hydrophobic patches, promoting aggregation. We noted that the concentration of Arg-HCl was not fully optimized, and further studies could be done to obtain the optimal conditions for elution with Arg-HCl as well as with other salts additives, which may help to improve the overall purity.

4.2 Effects of high molecular flexibility of aBsAb on Protein A chromatography

Although some form of flexibility of the aBsAb is desired for the binding to their intended therapeutic target, scFv linker length and flexibility has resulted in many problems in purification namely their tendency to form multimers, lowered thermal stability and scFv mediated aggregation [35]. Throughout our study, apart from the problem of chromatography-induced aggregation, we also observed a high degree of flexibility in the structure of the aBsAb, resulting in varying SEC—HPLC profiles. Mass spectrometry analysis confirmed that despite the different SEC profiles, the intact mass remained the same. This indicates the likelihood of structural flexibility, possibly originating from the GS linker between the Fc and scFv, and/or within the scFv domains. These GS linkers are noted for their flexibility and its stability is influenced by its length [36,37]. This variation in the hydrodynamic radius of the aBsAb leads to different SEC—HPLC profiles.

Furthermore, we noticed a distinct change in the hydrodynamic radius of the Protein A eluate after reacidification following neutralization, unlike traditional mAbs. This observation suggests that the structure of the aBsAb is flexible and pH-dependent, likely due to the presence of two flexible linkers attached to the scFv, which become more rigid after pH reduction.

The flexibility of the aBsAb continues to pose a problem during Protein A purification. Predictive models have shown how a protein's aggregation propensity can be correlated to its conformational flexibility and by reducing flexibility, the protein's aggregation propensity can be reduced [38-40]. Various methods protein engineering methods have been employed to stabilize the scFv domain including introducing disulfide bonds between VH and VL domains, and

adding two disulfide bonds between the scFv linker and the two variable domains to minimize scFv breathing, thereby improving their biophysical properties [35,41].

5 Conclusions

In conclusion, we investigated the effects of molecule hydrophobicity and structural flexibility of aBsAb on Protein A chromatography. We presented how its highly hydrophobic nature and structural flexibility led to increased aggregation. We also demonstrated with proper optimization, aBsAb can be purified with Protein A chromatography to a purity of 93 % and HMW less than 5 %. The structural flexibility of the scFv linkers to the parental antibody also resulted in different hydrodynamic sizes of the aBsAb molecule. The hydrodynamic radius of the aBsAb post Protein A neutralization and re-exposure to acid changed and was shown to be pH dependent. These results give an indication of how the complexity of these aBsAb affect the interactions between the column during purification and require more time for extensive study during development work.

[Instruction: The authorship contribution statement sections are duplicated.]CRediT authorship contribution statement

Xinhui Wang: Investigation, data curation, formal analysis, project administration, writing – original draft. Nattha Ingavat: Conceptualization, methodology, formal analysis, project administration, writing – review & editing. Liew Jia Min: Investigation. Nuruljannah Dzulkiflie: Discussion and analysis. Han Ping Loh: Investigation, writing – original draft. Yee Jiun Kok: Investigation, formal analysis, writing – original draft. Xuezhi Bi: Supervision. Yuansheng Yang: Supervision, Wei Zhang: Conceptualization, supervision, writing – review & editing.

CRediT authorship contribution statement

Xinhui Wang: Writing – original draft, Investigation, Formal analysis. **Nattha Ingavat:** Project administration, Investigation, Formal analysis. **Jia Min Liew:** Formal analysis, Data curation. **Nuruljannah Dzulkiflie:** Formal analysis. **Han Ping Loh:** Formal analysis, Data curation. **Yee Jiun Kok:** Formal analysis, Data curation. **Xuezhi Bi:** Supervision. **Yuansheng Yang:** Supervision. **Wei Zhang:** Writing – review & editing, Supervision, Resources, Project administration, Funding acquisition, Formal analysis, Conceptualization.

Declaration of competing interest

The authors declare that they have no known competing financial interests or personal relationships that could have appeared to influence the work reported in this paper.

Acknowledgments

This research was supported by Agency for Science, Technology, and Research (A*STAR) BMRC Central Research Fund.

Supplementary materials

Supplementary material associated with this article can be found, in the online version, at doi:10.1016/j.chroma.2024.465206.

References

The corrections made in this section will be reviewed and approved by a journal production editor. The newly added/removed references and its citations will be reordered and rearranged by the production team.

[1] Y. Sun, et al., Bispecific antibodies in cancer therapy: target selection and regulatory requirements, Acta Pharm. Sin. B 13 (9) (2023) 3583–3597, doi:10.1016/j.apsb.2023.05.023.

[2] S. Crescioli, et al., Antibodies to watch in 2024, MAbs. 16 (1) (2024) 2297450, doi:10.1080/19420862.2023.2297450.

[3] H. Kaplon, et al., Antibodies to watch in 2023, MAbs. 15 (1) (2023) 2153410, doi:10.1080/19420862.2022.2153410.

[4] U. Brinkmann, R.E. Kontermann, The making of bispecific antibodies, MAbs. 9 (2) (2017) 182–212, doi:10.1080/19420862.2016.1268307.

[5]

C. Spiess, Q. Zhai, P.J. Carter, Alternative molecular formats and therapeutic applications for bispecific antibodies, Mol. Immunol. 67 (2 Pt A) (2015) 95–106, doi:10.1016/j.molimm.2015.01.003.

[6] S.J. Keam, Cadonilimab: first Approval, Drugs 82 (12) (2022) 1333–1339, doi:10.1007/s40265-022-01761-9.

[7] M. Elshiaty, H. Schindler, P. Christopoulos, Principles and current clinical landscape of multispecific antibodies against cancer, Int. J. Mol. Sci. 22 (2021), doi:10.3390/ijms22115632.

[8] Q. Wang, et al., Design and production of bispecific antibodies, Antibodies (Basel) 8 (3) (2019), doi:10.3390/antib8030043.

[9] B. Husain, D. Ellerman, Expanding the boundaries of biotherapeutics with bispecific antibodies, BioDrugs 32 (5) (2018) 441–464, doi:10.1007/s40259-018-0299-9.

[10] C. Andrade, et al., An integrated approach to aggregate control for therapeutic bispecific antibodies using an improved three column Mab platform-like purification process, Biotechnol. Prog. 35 (1) (2019) e2720, doi:10.1002/btpr.2720.

[11] R. Glockshuber, et al., A comparison of strategies to stabilize immunoglobulin Fv-fragments, Biochemistry 29 (6) (1990) 1362–1367, doi:10.1021/bi00458a002.

[12] A. Worn, A. Pluckthun, Stability engineering of antibody single-chain Fv fragments, J. Mol. Biol. 305 (5) (2001) 989–1010, doi:10.1006/jmbi.2000.4265.

[13] G. Yuan, et al., Antibody aggregation can lead to reduced Protein A binding capacity and low step yield, Protein Expr. Purif. 210 (2023) 106315, doi:10.1016/j.pep.2023.106315.

[14] S.W. Chen, W. Zhang, Current trends and challenges in the downstream purification of bispecific antibodies, Antib. Ther. 4 (2) (2021) 73–88, doi:10.1093/abt/tbab007.

[15] A.M. McCall, et al., Isolation and characterization of an anti-CD16 single-chain Fv fragment and construction of an anti-HER2/neu/anti-CD16 bispecific scFv that triggers CD16-dependent tumor cytolysis, Mol. Immunol. 36 (7) (1999) 433–445, doi:10.1016/s0161-5890(99)00057-7.

[16] H.K. Ong, et al., Vector design for enhancing expression level and assembly of knob-into-hole based FabscFv-Fc bispecific antibodies in CHO cells, Antib. Ther. 5 (4) (2022) 288–300, doi:10.1093/abt/tbac025.

[17] N. Ingavat, et al., Harnessing ceramic hydroxyapatite as an effective polishing strategy to remove product- and process-related impurities in bispecific antibody purification, Bioresour. Bioprocess. 10 (1) (2023) 93, doi:10.1186/s40643-023-00713-9.

[18] M. Reth, Matching cellular dimensions with molecular sizes, Nat. Immunol. 14 (8) (2013) 765–767, doi:10.1038/ni.2621.

[19] P. Gagnon, R. Nian, Conformational plasticity of IgG during protein A affinity chromatography, J. Chromatogr. A 1433 (2016) 98–105, doi:10.1016/j.chroma.2016.01.022.

[20] P. Gagnon, et al., Transient conformational modification of immunoglobulin G during purification by protein A affinity chromatography, J. Chromatogr. A 1395 (2015) 136–142, doi:10.1016/j.chroma.2015.03.080.

[21] M. Zarrineh, et al., Mechanism of antibodies purification by protein A, Anal. Biochem. 609 (2020) 113909, doi:10.1016/j.ab.2020.113909.

[22] D. Moiani, et al., Structural characterization of a Protein A mimetic peptide dendrimer bound to human IgG, J. Phys. Chem. B 113 (50) (2009) 16268–16275, doi:10.1021/jp909405b.

[23] T.K. Cloutier, et al., Molecular computations of preferential interactions of proline, arginine.HCl, and NaCl with IgG1 antibodies and their impact on aggregation and viscosity, MAbs. 12 (1) (2020) 1816312, doi:10.1080/19420862.2020.1816312.

[24]

C. Munch, A. Bertolotti, Exposure of hydrophobic surfaces initiates aggregation of diverse ALS-causing superoxide dismutase-1 mutants, J. Mol. Biol. 399 (3) (2010) 512–525, doi:10.1016/j.jmb.2010.04.019.

[25] Q. Wu, et al., Decreasing hydrophobicity or shielding hydrophobic areas of CH2 attenuates low pH-induced IgG4 aggregation, Front. Bioeng. Biotechnol. 11 (2023), doi:10.3389/fbioe.2023.1257665.

[26] A.A. Shukla, P. Gupta, X. Han, Protein aggregation kinetics during Protein A chromatography. Case study for an Fc fusion protein, J. Chromatogr. A 1171 (1–2) (2007) 22–28, doi:10.1016/j.chroma.2007.09.040.

[27] T. Arakawa, et al., Elution of antibodies from a Protein-A column by aqueous arginine solutions, Protein Expr. Purif. 36 (2) (2004) 244–248, doi:10.1016/j.pep.2004.04.009.

[28] D. Ejima, et al., Effective elution of antibodies by arginine and arginine derivatives in affinity column chromatography, Anal. Biochem. 345 (2) (2005) 250–257, doi:10.1016/j.ab.2005.07.004.

[29] D. Shukla, et al., Understanding the role of arginine as an eluent in affinity chromatography via molecular computations, J. Phys. Chem. B 115 (11) (2011) 2645–2654, doi:10.1021/jp111156z.

[30] L. Gentiluomo, et al., Characterization of native reversible self-association of a monoclonal antibody mediated by fab-fab interaction, J. Pharm. Sci. 109 (1) (2020) 443–451, doi:10.1016/j.xphs.2019.09.021.

[31] R. Esfandiary, et al., Mechanism of reversible self-association of a monoclonal antibody: role of electrostatic and hydrophobic interactions, J. Pharm. Sci. 104 (2) (2015) 577–586, doi:10.1002/jps.24237.

[32] S.W. Chen, et al., Investigation of the effect of salt additives in Protein L affinity chromatography for the purification of tandem single-chain variable fragment bispecific antibodies, MAbs. 12 (1) (2020) 1718440, doi:10.1080/19420862.2020.1718440.

[33] C. Sudrik, et al., Preferential interactions of trehalose,L-arginine.HCl and sodium chloride with therapeutically relevant IgG1 monoclonal antibodies, MAbs. 9 (7) (2017) 1155–1168, doi:10.1080/19420862.2017.1358328.

[34] D. Shukla, B.L. Trout, Interaction of arginine with proteins and the mechanism by which it inhibits aggregation, J. Phys. Chem. B 114 (42) (2010) 13426–13438, doi:10.1021/jp108399g.

[35] L.E. Boucher, et al., Stapling" scFv for multispecific biotherapeutics of superior properties, MAbs. 15 (1) (2023) 2195517, doi:10.1080/19420862.2023.2195517.

[36] P.J. Hudson, A.A. Kortt, High avidity scFv multimers; diabodies and triabodies, J. Immunol. Methods 231 (1–2) (1999) 177–189, doi:10.1016/s0022-1759(99)00157-x.

[37] M. Arslan, et al., Effect of non-repetitive linker on in vitro and in vivo properties of an anti-VEGF scFv, Sci. Rep. 12 (1) (2022) 5449, doi:10.1038/s41598-022-09324-4.

[38] L. Galm, S. Amrhein, J. Hubbuch, Predictive approach for protein aggregation: correlation of protein surface characteristics and conformational flexibility to protein aggregation propensity, Biotechnol. Bioeng. 114 (6) (2017) 1170–1183, doi:10.1002/bit.25949.

[39] C. Zhang, et al., Computational Design To Reduce Conformational Flexibility and Aggregation Rates of an Antibody Fab Fragment, Mol. Pharm. 15 (8) (2018) 3079–3092, doi:10.1021/acs.molpharmaceut.8b00186.

[40] M. Valerio, et al., Early events in protein aggregation: molecular flexibility and hydrophobicity/charge interaction in amyloid peptides as studied by molecular dynamics simulations, Proteins. 58 (1) (2005) 110–118, doi:10.1002/prot.20306.

[41] U. Brinkmann, et al., A recombinant immunotoxin containing a disulfide-stabilized Fv fragment, Proc. Natl. Acad. Sci. U. S. A. 90 (16) (1993) 7538–7542, doi:10.1073/pnas.90.16.7538.

Highlights

- High molecule hydrophobicity causes chromatography-induced aggregation of aBsAb.
- Arg-HCl retards aBsAb elution from Protein A column rather than facilitating.
- High molecular flexibility leads to different hydrodynamic sizes of aBsAb molecule.
- Flexibility of the aBsAb molecule is pH dependent.
- aBsAb purity was improved from 29 % to 93 % by one-step Protein A with HMW<5 %.

Appendix Supplementary materials

Multimedia Component 1

alt-text: Image, application 1

Queries and Answers

Q1

Query: Please review the given names (no colouring) and surnames (highlighted in teal colouring) to make sure that we have identified them correctly and that they are presented in the desired order. Carefully verify the spelling of all authors' names as well. If changes are needed, please provide the edits in the author section.

Answer: Correct.

Q2

Query: Your article is registered as a regular item and is being processed for inclusion in a regular issue of the journal. If this is NOT correct and your article belongs to a Special Issue/Collection please contact s.prasannahm@elsevier.com immediately prior to returning your corrections.

Answer: Correct.

Q3

Query: [FND001] Correctly acknowledging the primary **funders and grant IDs** of your research is important to ensure compliance with funder policies. Please make sure that funders are mentioned accordingly.

Answer: Correct.